Bend-shear-mode instabilities of nematic liquid crystals in ac fields

Papiya Sengupta and Alfred Saupe
Liquid Crystal Institute and Physics Department, Kent State University, Kent, Ohio 44242
(Received 19 February 1974)

Hydrodynamic instabilities of nematic liquid crystals with a negative dielectric anisotropy in ac electric fields are theoretically studied. The instabilities considered are due to the development of bend modes coupled with flow fields of equal periodicity (Carr, Helfrich). A simple numerical procedure is developed which allows a convenient and exact calculation of threshold curves and instability regions which depend essentially only on two parameters, the reduced cutoff frequency and the reduced decay time of the bend-shear mode. Results of numerical calculations are presented in stability charts using reduced field and frequency coordinates. Characteristic features of threshold curves are discussed and a general survey is given on the position and the extent of instability regions.

I. INTRODUCTION

When a nematic liquid crystal is subjected to an external electric field, a hydrodynamic instability may be induced. In dc field normal isotropic liquids show similar instabilities as nematic liquid crystals. The dc instability is assumed to be due to unipolar charge injection at the electrodes.[1-3] The ac field instability has no corresponding effect in normal liquids. At a certain threshold voltage and below a cutoff frequency, cellular flow patterns are observed which are known as Williams domains.[4] At higher frequencies and higher voltages, another instability is observed with a different texture.[5] As suggested by Carr,[6] the anisotropy of conductivity is important for this ac instability. The first theoretical treatment of hydrodynamic instabilities on this basis was done by Helfrich.[7] The treatment was extended to include time-dependent solutions by Dubois-Violette, de Gennes, and Parodi.[8] They also present a comprehensive discussion of the types, conduction and dielectric regime, and general ranges of the instabilities based on approximate solutions. For the transition range where the approximations become unreliable, exact numerical calculations have been made for a 50-μm thick nematic film of methoxybenzalbutyloxyaniline (MBBA).[9] The boundaries in this calculation are taken into account approximately by setting an upper limit to the wavelength of the permitted bend-shear modes.

In this paper we reproduce the earlier results using a simple numerical procedure which allows a convenient calculation of bend-shear-mode instabilities and make additional calculations. The stability curves depend essentially only on the two parameters $\omega_c\tau_1$ and τ_1/τ_b, where ω_c denotes the cutoff frequency for the "conduction regime", τ_1 is the longitudinal dielectric relaxation time, and τ_b is the relaxation time for the bend mode. While ω_c and τ_1 are solely determined by material properties the (effective) τ_b can be modified by experimental conditions, e.g., by application of a magnetic field. The instability ranges are calculated for a number of selected sets of parameter values and the results presented in stability charts that give a general survey on the influence of the parameters.

The conduction regime has an upper voltage boundary at which the system returns to stability; we discuss the condition under which this return to stability may be experimentally observed. We also test in a particular example the first-order approximation for the conduction regime which is usually implied in experimental determinations of the cutoff frequency. It is found that this approximation may not be appropriate for this purpose in thin films (<50 μm for MBBA).

II. ASSUMPTIONS AND BASIC DIFFERENTIAL EQUATIONS

We investigate the instabilities of a uniformly aligned nematic liquid crystal in ac electric fields with respect to bend-shear modes. The starting equations are the torque balance equation for the director field, the equation of motion, and some fundamental electrodynamic equations. A detailed derivation has been given by DuBois-Violette *et al.*[8] We can limit ourselves, therefore, to a short outline in which we will emphasize the points of interest.

The director $\vec{n}$ of the unperturbed nematic is assumed parallel to the x axis of a Cartesian coordinate system and the applied electric field parallel to the z axis. Only modes of small amplitudes are considered and only first-order terms are retained. We can write accordingly for the

bend modes of interest $\vec{n} = 1, 0, \psi$ with

$$\psi = \phi_1 \cos qx, \quad \phi_1 \ll 1. \tag{1}$$

The torque-balance equation in the first approximation is

$$\gamma_1 \dot{\psi} + \left(k_{33} q^2 + \chi_a H^2 - \frac{\epsilon_a}{4\pi} E_z^2 \right) \psi - \frac{\epsilon_a}{4\pi} E_z E_x + \alpha_2 \frac{\partial \nu}{\partial x} = 0 . \tag{2}$$

Time derivatives here and in the following are indicated by a dot. γ_1 is the rotational viscosity of the directorfield, α_2 is a Leslie-Erickson viscosity coefficient which accounts for the frictional coupling between bend and shear modes, k_{33} is the bend elastic constant, $\epsilon_a = \epsilon_1 - \epsilon_2$ is the dielectric, and $\chi_a = \chi_1 - \chi_2$ is the diamagnetic anisotropy (1-direction $\parallel$ and 2-direction $\perp \vec{n}$). We admit that a static magnetic field is applied parallel to the x axis. In cases where it is applied in z direction, $\chi_a H^2$ has a negative sign in Eq. (2). For aromatic compounds $\chi_a > 0$, so that in the first case the field stabilizes the original alignment and in the second case destabilizes it.

We neglect the compressibility of the liquid and set $\mathrm{div}\vec{\nu} = 0$; no boundary effects are taken into account. The induced flow has, therefore, only a z component. The equation of motion becomes

$$\rho \dot{\nu} - \eta_1 \frac{\partial^2 \nu}{\partial x^2} - \alpha_2 \frac{\partial}{\partial x} \dot{\psi} - \rho_e E_z = 0 . \tag{3}$$

Here ρ is the mass density, ρ_e is the charge density and $\eta_1 = \frac{1}{2}(-\alpha_2 + \alpha_4 + \alpha_5)$ is the effective shear viscosity.

The inertial term $\rho\dot{\nu}$ can in general be neglected, in which case Eq. (3) gives $\partial^2\nu/\partial x^2$ as a linear function of ρ_e, and $\partial\dot{\psi}/\partial x$, which can be substituted in the derivated Eq. (2).

Furthermore, we have

$$4\pi\rho_e = \mathrm{div}\vec{D} = \epsilon_1 \frac{\partial E_x}{\partial x} + \epsilon_a E_z \frac{\partial \psi}{\partial x}, \tag{4}$$

which give $\partial E_x/\partial x$ as a function of ρ_E, $\partial\psi/\partial x$, and E_z.

Finally, for ρ_e we obtain

$$\dot{\rho}_e = -\mathrm{div} j = -\frac{1}{\tau_1}\left(\rho_e + Q_0 E_z \frac{\partial \psi}{\partial x} \right);$$

$$Q_0 = \frac{\epsilon_2}{4\pi}\left(1 - \frac{\tau_1}{\tau_2} \right); \quad \tau_i = \frac{\epsilon_i}{4\pi\sigma_i}; \quad i = 1, 2. \tag{5}$$

Here σ_1 and σ_2 denote the principle conductivities, and τ_1 and τ_2 are the decay times for space charges. Q_0 determines the equilibrium charge distribution for a given field E_z and ψ. Using Eqs. (5), (4), and (3), we obtain from Eq. (2) (neglecting $\rho\dot{\nu}$)

$$\frac{\partial}{\partial x}\left(\dot{\psi} + \frac{1}{\tau_b}\psi + \frac{\theta}{\eta_b} E_z^2 \psi \right) + \frac{\tau_1}{\eta_b} Q_1 \dot{\rho}_e E_z = 0 ;$$

$$\eta_b = \gamma_1 - \frac{\alpha^2}{\eta_1}; \quad \tau_b = \eta_b/(k_{33}q^2 + \chi_a H^2); \tag{6}$$

$$Q_1 = \frac{\epsilon_a}{\epsilon_1} + \frac{\alpha_2}{\eta_1}; \quad \theta = Q_0 Q_1 - \frac{\epsilon_a \epsilon_2}{\epsilon_1 4\pi},$$

η_b is the viscosity coefficient of the bend-shear mode and τ_b is its decay time. The coefficient θ, known as Helfrich parameter, determines the stability of the system. This can be easily seen when the last term proportional to $\dot{\rho}_e$ is neglected. As η_b is always positive, the sign of the torque due to the electric field is given by the sign of θ. The field, therefore, always stabilizes the alignment unless $\theta < 0$.

Neglecting the last term is justified only for certain limiting cases. But, judging from numerical results, the conclusion seems to be generally true when $\epsilon_a < 0$.

In case of dc fields, both terms involving time derivatives can be neglected and we obtain for the threshold field simply

$$E_z^2 = -(k_{33}q^2 + \chi_a H^2)/\theta . \tag{7}$$

III. STABILITY CHARTS

In the limit of small amplitudes we may write for the charge distribution

$$\rho_e = -qQ_0 E_0 \phi_2 \sin qx . \tag{8}$$

Together with the definition (1) and with $E_z = E_0 \times \cos\omega t$, Eqs. (5) and (6) lead to the following system of coupled differential equations for the amplitudes ϕ_1 and ϕ_2:

$$\tau_1\dot{\phi}_1 + [(\tau_1/\tau_b) - 2(\omega_c\tau_1)^2 e^2 \cos^2\omega t]\phi_1 + 2[1 + (\omega_c\tau_1)^2]e^2 \cos\omega t\, \tau_1\dot{\phi}_2 = 0,$$

$$\tau_1\dot{\phi}_2 + \phi_2 + \cos\omega t\,\phi_1 = 0. \tag{9}$$

Following the earlier treatment,[8] we have introduced a reduced "field" e and a cutoff frequency ω_c defined by:

$$e^2 = -\frac{\tau_1}{\eta_b}\frac{\epsilon_a}{\epsilon_1}\frac{\epsilon_2}{4\pi}\frac{E_0^2}{2};$$

$$(\omega_c\tau_1)^2 = \frac{\epsilon_1}{\epsilon_a}\left(1 - \frac{\tau_1}{\tau_2} \right)\left(\frac{\epsilon_a}{\epsilon_1} + \frac{\alpha_2}{\eta_1} \right) - 1 . \tag{10}$$

The cutoff frequency is related to the Helfrich parameter $\theta = \epsilon_2\epsilon_a(\omega_c\tau_1)^2/4\pi\epsilon_1$. It remains to calculate threshold fields as a function of the frequency and to study the dependence on the param-

eters τ_1/τ_b and $\omega_c\tau_1$. The third parameter, τ_1 itself, can be eliminated by the introduction of a reduced time t/τ_1. The threshold curves plotted against $\omega\tau_1$ form, therefore, a two-parametric family of curves.

Equations (9) form a system of linear differential equations with periodic coefficients. From the theory of differential equations (Floquet theorem[10]), it is known that there are two independent solutions of which at least one can be written in the form

$$\phi_j = e^{\mu t}\sum_\nu a_{j\nu}e^{i\nu\omega t}\,, \quad j=1,2\,. \tag{11}$$

Here μ is a characteristic exponent of which the imaginary part corresponding to the periodicity of the system is determined only modulo ω. For $\mathrm{Re}\,\mu > 0$ the amplitudes increase in time (instability); for $\mathrm{Re}\,\mu < 0$ the amplitudes decrease (stability). The boundaries or thresholds are obtained for $\mathrm{Re}\,\mu = 0$. In general, there are two different characteristic exponents with different $\mathrm{Re}\,\mu$, and to each one belongs a solution of the form (11).

With μ its conjugate complex $\mu^\dagger$ is also a characteristic exponent because the coefficients of (9) are real. There are no more than two essentially different exponents and we conclude, also using the relations (12), that generally $\mathrm{Im}\,\mu = n\omega$ with n integer. Without loss of generality we can, therefore, assume $\mathrm{Im}\,\mu = 0$.

It can be directly verified that with $\phi_1(t)$, $\phi_2(t)$, the functions $\phi_1[t+(\pi/\omega)]$, $-\phi_2[t+(\pi/\omega)]$ are also solutions. This ensures that the solutions of the form (11) suffice directly or can be modified to suffice one of the following relations:

$$a_{1,2\nu+1} = a_{2,2\nu} = 0\,, \tag{12a}$$

$$a_{1,2\nu} = a_{2,2\nu+1} = 0; \quad \nu = \pm1, \pm2, \pm3\ldots\,. \tag{12b}$$

In the first case the series for the bend mode contains only even-indexed coefficients; the second case contains only odd-indexed coefficients ($\mathrm{Im}\,\mu = 0$). Referring to the bend mode, we will in the following differentiate accordingly between even (12a) and odd (12b) solutions, or simply speak of even and odd modes. The even solutions incorporate the instability known as "conduction" regime; the odd solutions on the other hand incorporate the "dielectric" regime.

Using the form (11) of the solutions, we can obtain the following recurrency equation:

$$M_{\nu,\nu-1}a_{1,\nu-2} + M_{\nu,\nu}a_{1,\nu} + M_{\nu,\nu+1}a_{1,\nu+2} = 0\,,$$

$$M_{\nu,\nu} = (\tau_1/\tau_b) + (\mu + i\nu\omega)\tau_1 + M_{\nu,\nu-1} + M_{\nu,\nu+1}\,, \tag{13}$$

$$M_{\nu,\nu\pm1} = \frac{e^2}{2}\left(1 - \frac{1+(\omega_c\tau_1)^2}{1+\mu\tau_1+i(\nu\pm1)\omega\tau_1}\right)\,.$$

The three-term recurrency equation can be numerically solved using the method of continued fractions[11] (see the Appendix). Convergent solutions exist only for suitable sets of parameter values. This condition gives for $\mu = 0$ the threshold field as functions of the parameters $\omega\tau_1$, $\omega_c\tau_1$ and τ_1/τ_b.

IV. NUMERICAL RESULTS

We limit our calculations to the range of positive e^2 in which the instabilities of physical interest occur with materials of a negative dielectric anisotropy. Instabilities in the range of negative e^2 are of interest for materials with positive anisotropy which will not be considered in this paper.

A. Even modes

For even modes, a useful first-order approximation exists. It is obtained by setting $M_{0,0} = 0$ and is valid when the off-diagonal terms $M_{\nu,\nu\pm2}$ are small against $M_{\nu,\nu}$ for $|\nu| \geq 2$, as is true for

$$|e^2| \ll \frac{4\omega\tau_1|1+\mu\tau_1|}{2+|\omega_c\tau_1|^2+|\mu\tau_1|}\,. \tag{14}$$

In first order we thus obtain

$$e^2 = \left(\mu\tau_1 + \frac{\tau_1}{\tau_b}\right)\frac{(1+\mu\tau_1)^2+(\omega\tau_1)^2}{(\omega_c\tau_1)^2-(\omega\tau_1)^2-\mu\tau_1[1+\mu\tau_1+(\omega_c\tau_1)^2]}\,. \tag{15}$$

Equation (15) can be used for a discussion of the time dependence of the amplitude of the mode. For small values of μ and for frequencies not too close to ω_c, Eq. (15) gives

$$\mu = \frac{e^2}{\tau_1}\frac{(\omega_c\tau_1)^2-(\omega\tau_1)^2}{1+(\omega\tau_1)^2} - \frac{1}{\tau_b}\,. \tag{15'}$$

We see that for $\omega < \omega_c$ the conduction-induced effects dominate and the electric field is destabilizing. Above the threshold μ turns positive and the bend-mode formation begins. The value of μ and the speed of formation increases with the field in the first-order approximation. Exact calculations show the existence of an upper boundary for the even-instability range. The exponent μ, therefore, reaches a maximum for some finite field value.

When $\omega > \omega_c$ the dielectric torque dominates and the field stabilizes. The stabilizing effect increases with the frequency until for $\omega \gg \omega_c$ only the dielectric torque remains.

For $\mu = 0$, Eqs. (15) and (15′) are equal to the earlier derived approximation for the threshold.[8] In Fig. 1 the top part shows a set of threshold curves calculated in higher order for $\omega_c\tau_1 = 1.41$ and a number of different τ_1/τ_b values. The area to the left of each curve corresponds to the region of instability. The bottom part of Fig. 1 shows the

same threshold curves calculated in a first-order approximation. The comparison shows that in the given example the agreement is good in the range $e < 0.3$. (Other deviations which are not indicated in the figures occur at very low frequencies.) For small ratios $|\tau_1/\tau_b|$ the first-order approximation can be used even in the neighborhood of the cutoff frequency.

For negative τ_1/τ_b ratios the horizontal alignment is instable in the absence of an electric field. Such an instability can be produced by a vertical magnetic field. As mentioned, electric fields with $\omega > \omega_c$ have a stabilizing effect with respect to even disturbances. Stability exists above the threshold curves (a) in this range. At frequencies $\omega \gg \omega_c$ the curves approach the horizontal $e^2 = -\tau_1/\tau_b$, which gives explicitly

$$k_{33}q^2 - \chi_a H^2 - \frac{\epsilon_a \epsilon_2}{4\pi\epsilon_1}\frac{E_0^2}{2} = 0 . \tag{16}$$

The relation (16) gives the Fredericks threshold for bend modes with vertically applied magnetic and electric fields. The raise of the threshold curves when ω approaches ω_c from the high-frequency side is due to the formation of space charges. In thin films it is in fact possible to obtain Williams domains in this way for frequencies with $\omega > \omega_c$.

In the absence of a magnetic field, τ_1/τ_b is always positive. The least-stable mode is the one with the largest τ_b which is assumed for $q \to 0$. The mode that develops first assumes accordingly the largest wavelength compatible with the experimental conditions.

Many experimental observations are made in thin nematic films of a horizontal alignment with the field perpendicular to the layer. The effect of the boundaries[7,8] can be approximately accounted for by assuming that for permitted modes

$$q \geq \pi/d . \tag{17}$$

Exact calculations for thin films in the dc field[12,13] show the limits of this assumption, but we may still use it for our more qualitative con-

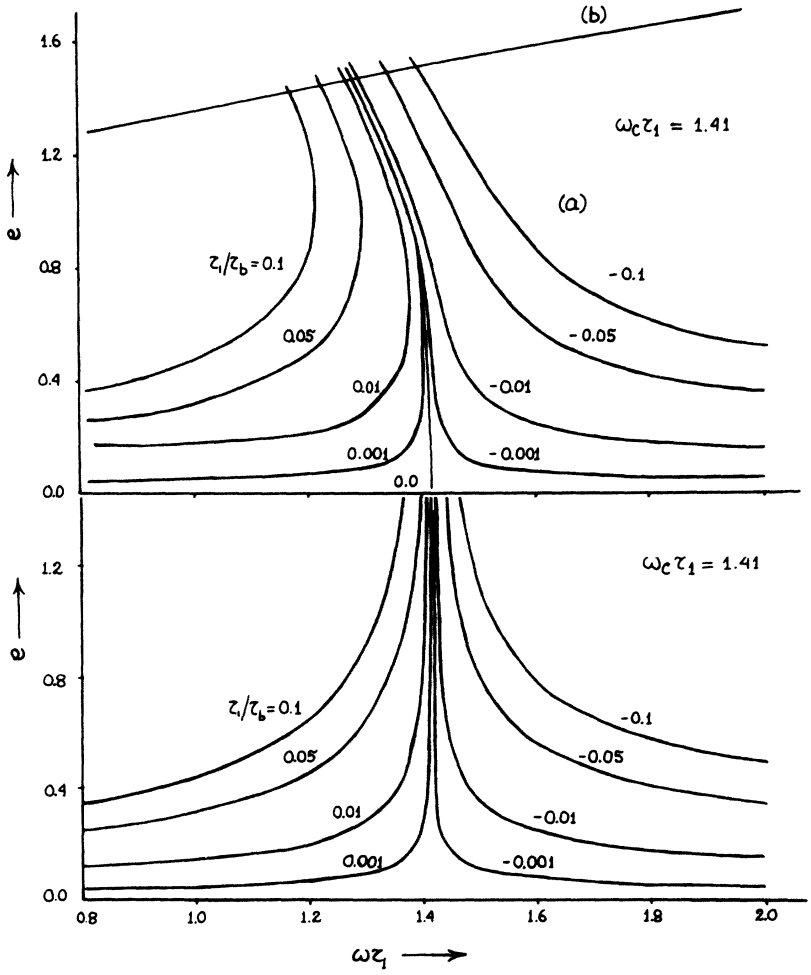

FIG. 1. Comparison of stability charts: (i) Top half—threshold fields in higher-order approximation: (a) even mode for selected values of τ_1/τ_b; (b) envelope of odd modes gives minimum threshold (τ_1/τ_b varies). (ii) Bottom part—threshold field of even modes in first-order approximation.

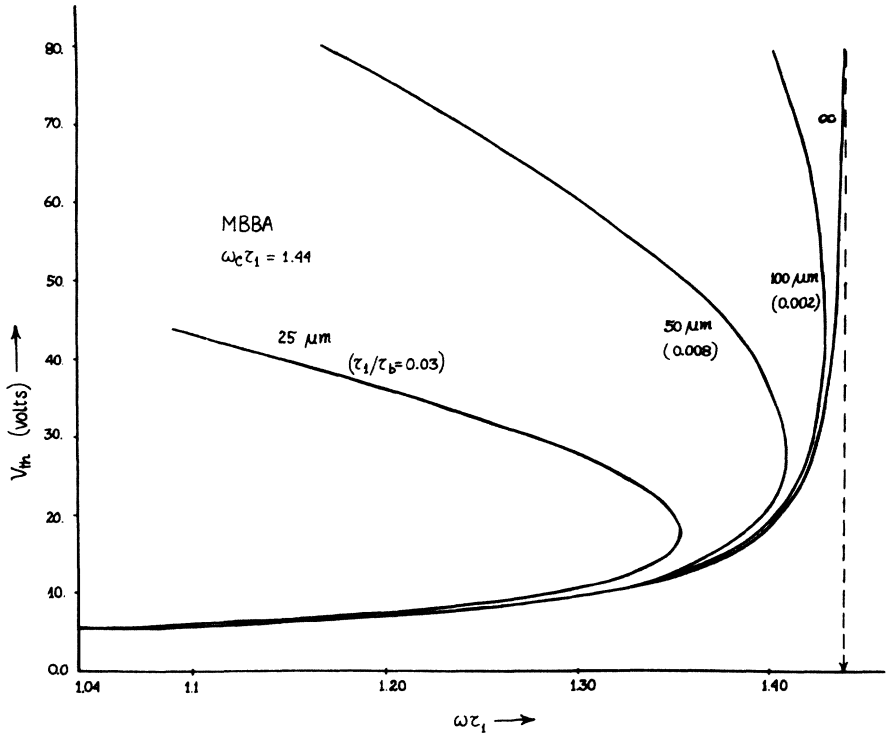

FIG. 2. Threshold voltage of even modes (conduction regime) calculated for different sample thickness ($H=0$). The selected material constants are typical for MBBA.

siderations.

Using Eq. (17), the experimental threshold curves in the conduction regime as observed in thin films should be compared with the theoretical curves calculated with $q=\pi/d$. In the first approximation without a magnetic field, the threshold voltage ($V=E_0 d/\sqrt{2}$ is then independent of the film thickness. Figure 2 shows the results obtained with this assumption for material parameter values corresponding to nematic liquid MBBA (methoxybenzalbutyloxyaniline) and $H=0$. The first-order approximation becomes accurate for

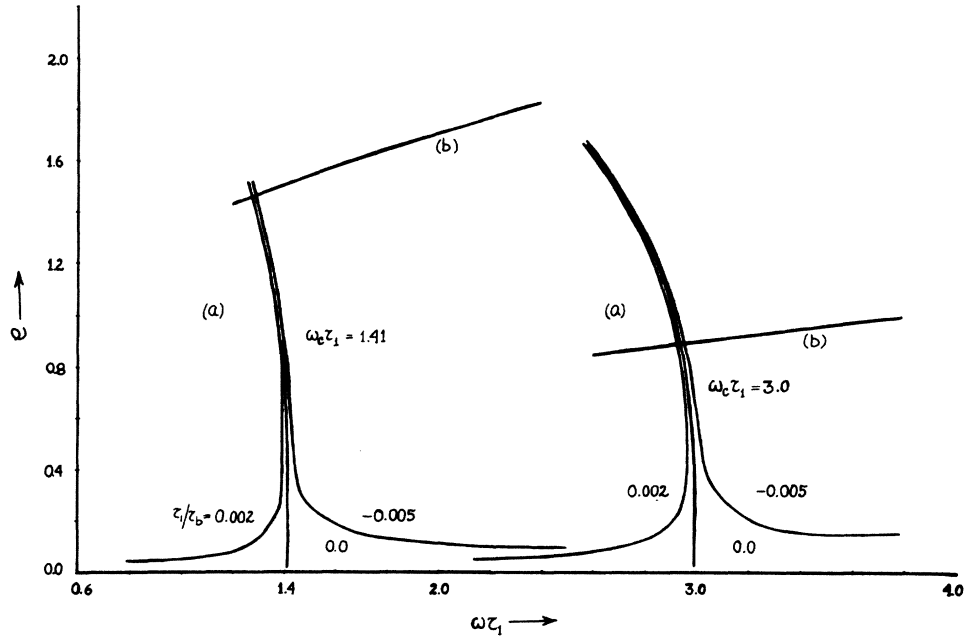

FIG. 3. Threshold field dependence on $\omega_c\tau_1$: (a) even modes; (b) envelope of odd modes.

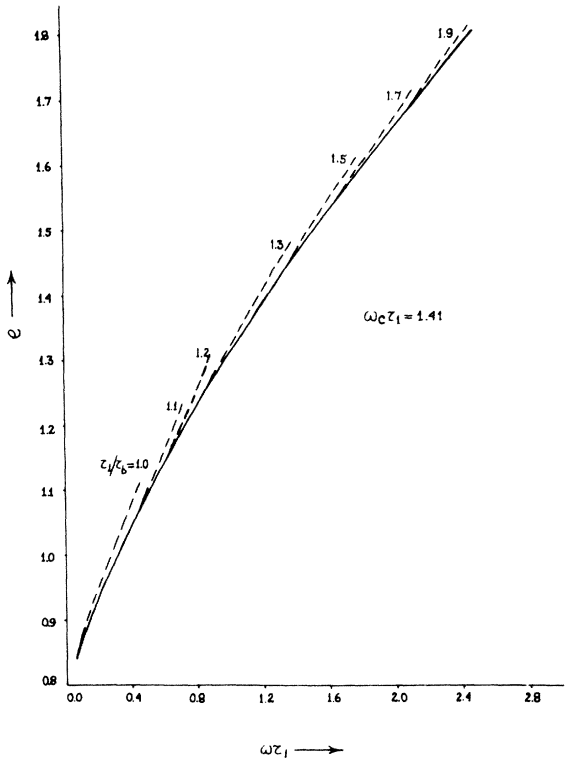

FIG. 4. Odd modes. Dashed curves give threshold for selected values of τ_1/τ_b; solid curve indicates envelope.

$d \to \infty$. There exists then a true cutoff frequency which is equal to ω_c. For finite d, or more accurately for $\tau_1/\tau_b > 0$, the curves turn back. The conduction-regime instability has an upper limit. In most experiments the upper limit cannot be observed as the odd-mode instability interferes.

In the presence of a strong stabilizing magnetic field when $\chi_a H^2 \gg K_{33}(\pi/d)^2$, practically a thickness-independent threshold field exists because the magnetic field determines τ_b and the restriction (17) has only negligible effects on the value of τ_b.

The dependence of the threshold on $\omega_c\tau_1$ is demonstrated in Fig. 3. The even solutions give similar sets of curves for different $\omega_c\tau_1$. The main change corresponds to a change of the $\omega\tau_1$ scale.

B. Odd modes

Figure 4 shows results calculated for odd modes. The dashed lines indicate the threshold curves for different fixed ratios τ_1/τ_b but the same $\omega_c\tau_1$. The solid line is the envelope. The calculated curves show no singularities around the cutoff frequency nor in another frequency range.

In contrast to the case described in Sec. IV A, the threshold at a fixed frequency is not a monotonic function of τ_1/τ_b in this case, but reaches a minimum for a finite positive value. In experiments the conditions are usually such that the

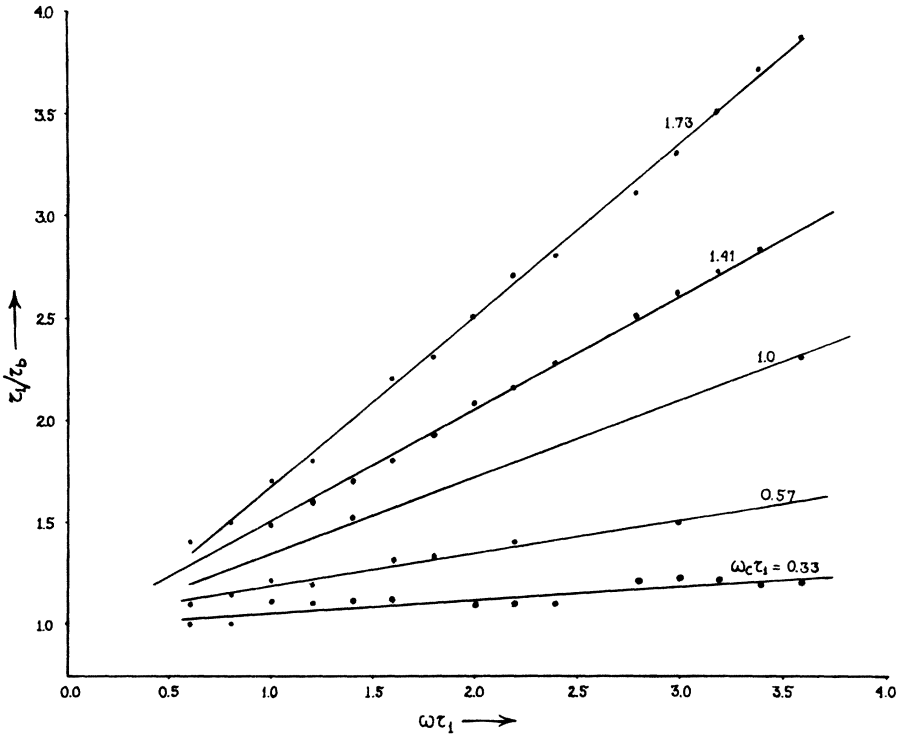

FIG. 5. Dependence of τ_1/τ_b on $\omega_c\tau_1$ along envelope of odd modes (points indicating the calculated values, the scattering corresponds to the error in their determination).

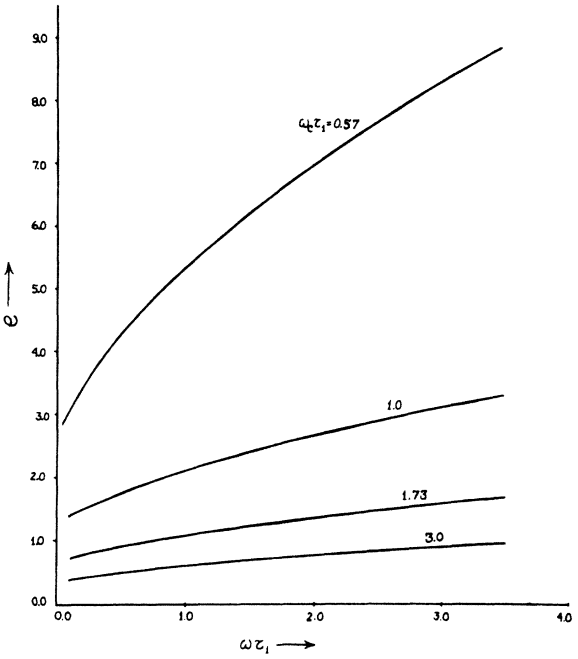

FIG. 6. Envelopes of odd modes for selected cutoff frequencies.

minimum is reached for a permitted $q \geq \pi/d$ so that boundary effects can be neglected. The observable threshold is in such cases given by the envelope.

The threshold is independent of a magnetic field, since it induces merely a change of q so that τ_b remains constant. Measurement of q as a function of H can, therefore, be used to determine the ratio k_{33}/χ_a but the results may be affected by the diffusion current.[8,14] Figure 5 shows that the dependence of τ_1/τ_b on the frequency in the studied frequency range is practically linear. The slope depends on $\omega_c\tau_1$; it becomes steeper for larger values of the parameter.

The threshold field dependence on $\omega_c\tau_1$ is presented in Fig. 6. The field increases with decreasing $\omega_c\tau_1$ and in the limit $\omega_c\tau_1 \to 0$ approaches the vertical line $\omega\tau_1 = 0$. The dependence differs strongly from the $\omega_c\tau_1$ dependence of the even solutions.

V. DISCUSSION

The comparison between experimental and calculated curves is only possible to a limited extent, since in regions of overlapping instability regimes only the lowest threshold can be readily observed. For this reason, the upper-instability border for the conduction regime was not found experimentally in sinusoidal electric field with MBBA and PAA. It is, therefore, of interest to discuss under which conditions the return to stability can be best observed and what material properties are most favorable.

In Fig. 7 calculated stability curves assuming material constants typical for MBBA and PAA are compared. The graphs show that the conditions for MBBA are more favorable. In general we find (see Fig. 8) that at a given τ_1/τ_b the intersection between the threshold curves moves further away from the apex with decreasing $\omega_c\tau_1$. The upper boundary and the return to stability has been in fact observed recently with a compound of a strong

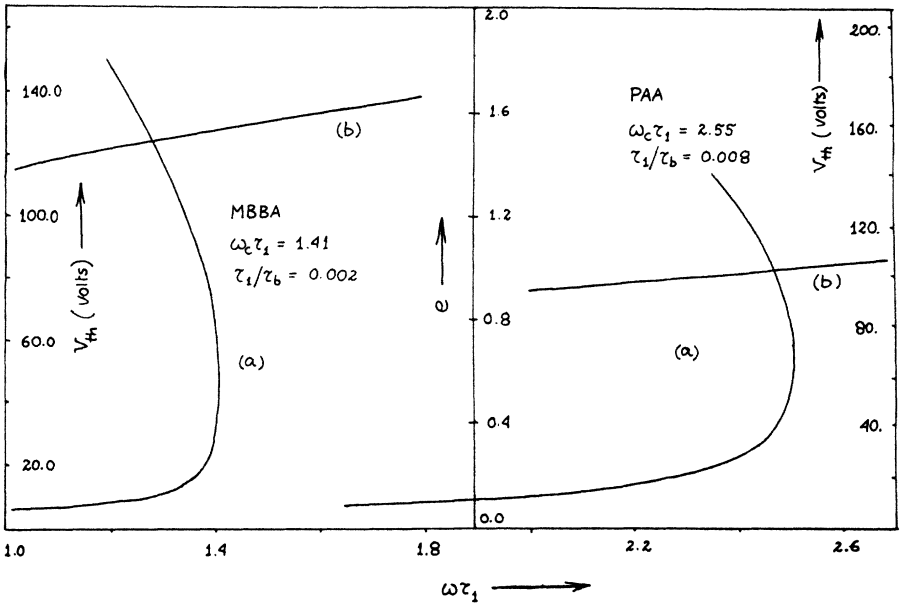

FIG. 7. Threshold fields typical for MBBA and PAA: (a) even mode (conduction regime), τ_1/τ_b corresponding to a 100 μm thick film with $H = 0$; (b) envelope of odd modes.

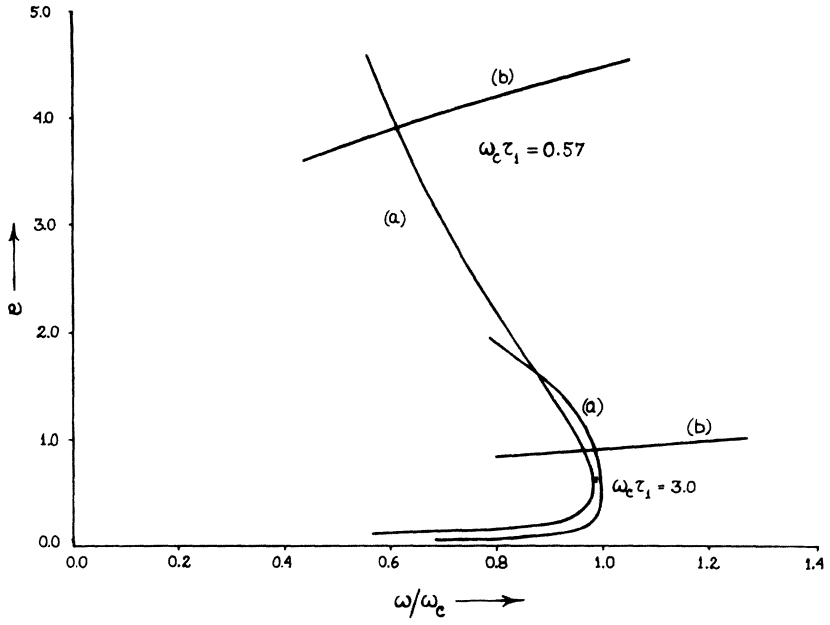

FIG. 8. Threshold fields against ω/ω_c: (a) even modes for $\tau_1/\tau_b = 0.002$; (b) envelopes of odd modes.

negative anisotropy[15] for which accordingly $\omega_c\tau_1$ is likely to be much smaller than for MBBA.

As we have mentioned, the curve of the conduction regime, and the even threshold curve in general, can only approximately agree with the curves observed in thin films because of the boundary effects. For the odd-threshold curves boundary conditions are usually without influence, but here the validity is limited due to the diffusion current which becomes important when the wavelength of the mode is comparable to the diffusion length of the charge carrier in the time τ_1.[8] It may cause considerable deviations at relatively low frequencies. These limitations should be kept in mind when the graphs are used for a survey on the variation of the stability curves with experimental conditions and with material properties.

APPENDIX

The three-term recurrency equation (13) can conveniently be solved using the method of continued fractions.[11] We rewrite Eq. (13) in the form

$$\frac{a_{1,\nu}}{a_{1,\nu\pm2}} = -\frac{M_{\nu,\nu\mp2}}{M_{\nu,\nu}+M_{\nu,\nu\pm2}(a_{1,\nu\pm2}/a_{1,\nu})} . \tag{18}$$

For a convergent series and for a large enough positive value n, we may neglect $M_{\pm n,\pm(n+2)}(a_{1,\pm(n+2)}/a_{1,\pm n})$ against $M_{\pm n,\pm n}$. (For large $|\nu|$, $M_{\nu,\nu}\sim i\nu\omega\tau_1$, while $M_{\nu,\nu\pm2}\sim e^2/2$). This allows the following procedure:

For a given set of parameter values $\omega\tau_1$, $\omega_c\tau_1$, τ_1/τ_b, and e^2, and for a large number n, we start with

$$R_{\pm n} = -M_{\pm n,\pm(n+2)}/M_{\pm n,\pm n} \tag{19}$$

and calculate successively $R_{\pm\nu}$ for $0<\nu<n$ using (18), replacing $a_{1,\pm\nu}/a_{1,\pm(\nu-2)}$ by $R_{\pm\nu}$. The calculations are carried down to $\nu=2$ for the even series (n even) or to $\nu=1$ for the odd series (n odd). For a compatible set of parameter values, we have

$$\begin{aligned} &M_{0,-2}R_{-2}+M_{0,0}+M_{0,2}R_2 = 0 \quad (n \text{ even}), \\ &R_{-1}R_1 = 1 \qquad\qquad\qquad\quad (n \text{ odd}). \end{aligned} \tag{20}$$

Equations (20) are in general not fulfilled. A suitable parameter, e.g., e^2 or $\omega\tau_1$, has then to be varied until the condition is met. Setting $\mu = 0$, one can thus easily calculate the boundaries of instability ranges.

A Burrough 5500 computer has been used for the numerical analysis. The program is written in Fortran and we have used a simple iterative procedure. For the calculations, we set $n=50$ (even series) and $n=51$ (odd series), although results are practically independent of n for $n>10$.

[1]N. Felici, Revue Generale d'Electricité 78, 717 (1969).
[2]P. G. de Gennes, Comm. Solid State Phys. 3, 35 (1970).
[3]Orsay Liquid Crystal Group, Phys. Rev. Lett. 25, (24), 1642 (1970).
[4]R. Williams, J. Chem. Phys. 39, 384 (1963).
[5]G. Heilmeier and W. Helfrich, Appl. Phys. Lett. 16, 1955 (1970).
[6]E. F. Carr, Mol. Cryst. Liq. Cryst. 7, 253 (1969).
[7]W. Helfrich, J. Chem. Phys. 51, 4092 (1969).
[8]E. Dubois-Violette, P. G. de Gennes, and O. Parodi, J. Phys. (Paris) 32, 305 (1971).
[9]E. Dubois-Violette, J. Phys. (Paris) 33, 95 (1972).
[10]L. Cessari, *Asymptotic Behaviour and Stability Problems in Ordinary Differential Equations* (Academic, New York, 1963), Chap. 2, p. 55.
[11]P. M. Morse and H. Feschback, *Methods of Theoretical Physics* (McGraw-Hill, New York, 1953), Part 1, Chap. 5, p. 557.
[12]P. A. Penz,and G. W. Ford, Phys. Rev. A 6, 414 (1972).
[13]P. Sengupta, W. Franklin, and A. Saupe (to be published).
[14]Orsay Liquid Crystal Group, Mol. Cryst. Liquid Cryst. 12, 251 (1971).
[15]W. de Jeu and J. Van der Veen, Phys. Lett. A 44, 4 (1973).